Received: 8 March 2019 | Revised: 18 July 2019 | Accepted: 22 July 2019

DOI: 10.1002/mrm.27942

RAPID COMMUNICATION

Magnetic Resonance in Medicine

Natively fat-suppressed 5D whole-heart MRI with a radial free-running fast-interrupted steady-state (FISS) sequence at 1.5T and 3T

Jessica A.M. Bastiaansen[1] | **Davide Piccini**[1,2] | **Lorenzo Di Sopra**[1] | **Christopher W. Roy**[1] | **John Heerfordt**[1,2] | **Robert R. Edelman**[3,4] | **Ioannis Koktzoglou**[3,5] | **Jérôme Yerly**[1,6] | **Matthias Stuber**[1,6]

[1]Department of Diagnostic and Interventional Radiology, Lausanne University Hospital and University of Lausanne, Lausanne, Switzerland

[2]Advanced clinical imaging technology, Siemens Healthcare AG, Lausanne, Switzerland

[3]Department of Radiology, NorthShore University HealthSystem, Evanston, Illinois

[4]Northwestern University Feinberg School of Medicine, Chicago, Illinois

[5]The University of Chicago Pritzker School of Medicine, Chicago, Illinois

[6]Center for Biomedical Imaging, Lausanne, Switzerland

Correspondence
Jessica A.M. Bastiaansen, Department of Diagnostic and Interventional Radiology, University Hospital Lausanne (CHUV), Rue de Bugnon 46, BH 8.84, 1011 Lausanne, Switzerland.
Email: jbastiaansen.mri@gmail.com
Twitter: @Jessica_B_

Funding information
J.A.M.B.: Swiss National Science Foundation, grant number PZ00P3_167871; Emma Muschamp Foundation and Swiss Heart Foundation. M.S.: Swiss National Science Foundation, grant numbers 173129, 150828, and 143923. R.R.E.: National Institutes of Health, grant numbers R01 HL130093 and R01 HL137920. I.K.: National Institutes of Health, grant number R01 EB027475.

Purpose: To implement, optimize, and test fast interrupted steady-state (FISS) for natively fat-suppressed free-running 5D whole-heart MRI at 1.5 tesla (T) and 3T.

Methods: FISS was implemented for fully self-gated free-running cardiac- and respiratory-motion-resolved radial imaging of the heart at 1.5T and 3T. Numerical simulations and phantom scans were performed to compare fat suppression characteristics and to determine parameter ranges (number of readouts [NR] per FISS module and TR) for effective fat suppression. Subsequently, free-running FISS data were collected in 10 healthy volunteers and images were reconstructed with compressed sensing. All acquisitions were compared with a continuous balanced steady-state free precession version of the same sequence, and both fat suppression and scan times were analyzed.

Results: Simulations demonstrate a variable width and location of suppression bands in FISS that were dependent on TR and NR. For a fat suppression bandwidth of 100 Hz and NR ≤ 8, simulations demonstrated that a TR between 2.2 ms and 3.0 ms is required at 1.5T, whereas a range of 3.0 ms to 3.5 ms applies at 3T. Fat signal increases with NR. These findings were corroborated in phantom experiments. In volunteers, fat SNR was significantly decreased using FISS compared with balanced steady-state free precession ($P < 0.05$) at both field strengths. After protocol optimization, high-resolution (1.1 mm^3) 5D whole-heart free-running FISS can be performed with effective fat suppression in under 8 min at 1.5T and 3T at a modest scan time increase compared to balanced steady-state free precession.

Conclusion: An optimal FISS parameter range was determined enabling natively fat-suppressed 5D whole-heart free-running MRI with a single continuous scan at 1.5T and 3T, demonstrating potential for cardiac imaging and noncontrast angiography.

KEYWORDS
1.5T MRI, 3T MRI, bSSFP, compressed sensing, fat suppression, FISS, free-running, noncontrast, 3D radial, whole-heart MRI

1 | INTRODUCTION

Whole-heart 3D imaging approaches that are free-breathing and non-electrocardiogram (ECG)–triggered (i.e., free-running) are gaining in popularity because they reduce scanning complexity[1] by removing the need for specific slice orientations, gating, triggering, and in some cases even ECG lead placement.[2,3] Cardiac images can then be retrospectively reconstructed in arbitrary spatial and temporal dimensions and provide information on both cardiac anatomy and function from 1 single acquisition.[4]

In currently proposed free-running approaches, the manner in which high SNR and contrast are generated is field strength-dependent, with balanced steady-state free precession (bSSFP) being used for applications at 1.5T[1,4] and gradient-echo (GRE) sequences in combination with contrast agents at 3T.[2] Both methods achieved high spatial and temporal resolution using flexible radial sampling but reported lengthy scan durations of over 14 and 10 min, respectively. The application of advanced reconstruction methods such as XD-GRASP[5] on data acquired with free-running bSSFP[1] significantly improved cardiac image quality, but the scan durations remained over 14 min.[1,4] For visualization of certain anatomical structures, including the coronary arteries, fat suppression is mandatory. At 1.5T, this was performed using fat saturation prepulses that periodically interrupted the steady-state magnetization in bSSFP.[1] However, fat saturation in combination with mandatory ramp-up pulses remains relatively time-inefficient, and the water–fat cancellation artifact could still be observed at some of the coronary vessel borders.[1] As an alternative, the free-running postcontrast GRE approach at 3T used water excitation pulses to suppress fat signals,[2] which increases TR and may not be practical in combination with bSSFP. For the above reasons, there is a need for a time-efficient free-running method that incorporates homogeneous fat suppression that works at both 1.5T and 3T, that provides blood-muscle contrast, and for which contrast agent is an option but not a requirement.

Recently, a 2D radial fast interrupted steady-state (FISS) sequence has been developed that provides the high SNR and blood-muscle contrast-to-noise ratio of bSSFP while simultaneously suppressing fat under certain conditions.[6] FISS provides native fat suppression because the RF excitation pulses used for imaging simultaneously help suppress fat signal. In a free-running context, a FISS implementation may therefore lead to natively fat-suppressed imaging without needing periodically applied fat suppression and ramp-up pulses, which will be conducive of improved time efficiency and visualization of anatomical structures embedded in epicardial fat.

The above advances the hypothesis that a carefully optimized 3D version of FISS may be exploited for time-efficient fat-suppressed respiratory and cardiac motion-resolved free-running whole-heart imaging. Therefore, the purpose of this study was to 1) develop and implement a 3D radial FISS sequence as part of a fully self-gated free-breathing cardiac and respiratory motion-resolved 5D imaging framework, 2) provide a thorough analysis of native fat suppression capabilities of FISS within this framework by using numerical simulations and phantom experiments, 3) provide parameter ranges for free-running fat-suppressed imaging to be effective at 1.5T and 3T, and 4) demonstrate its feasibility for natively fat-suppressed whole-heart imaging at both field strengths in a single continuous scan and while comparing the results with those from a non–fat-suppressed free-running bSSFP acquisition.

2 | METHODS

2.1 | Theory

A FISS sequence can be viewed as an interrupted version of a bSSFP sequence[6] and can be combined with radial as well as Cartesian sampling patterns. These fast interruptions of a bSSFP echo train (Figure 1A) induce broad signal suppression bands, the location of which—and the bandwidth (BW) of which—are highly dependent on the TR and the frequency of the interruptions. The fat-suppressing properties of FISS and corresponding sequence parameters were thoroughly investigated in this study. In an earlier report,[6,7] FISS demonstrated a reduction in both flow artifacts compared with bSSFP and decreased arterial signal saturation relative to GRE. Another advantage of FISS with respect to bSSFP includes reduced signal oscillations from off-resonant tissues when approaching the steady state.[8]

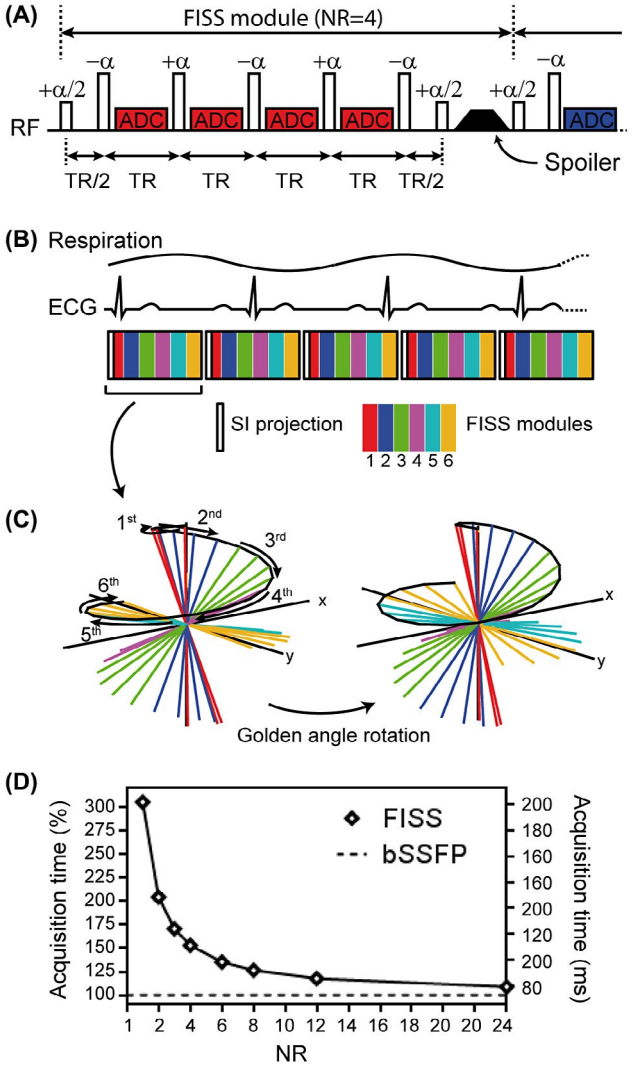

FIGURE 1 Sequence diagram illustrating the components within a FISS module (A). Each FISS module starts with a tip-down pulse of α/2, is followed by RF excitation pulses of which the number depends on the amount of readouts per FISS module (NR), and ends with a tip-up pulse α/2. After each FISS module the magnetization is spoiled, and each RF pulse, regardless of NR, is phase alternated by 180°. RF spoiling by 117 degrees is applied across FISS modules. Within a free-running framework, FISS is implemented as a free-breathing and non-ECG-triggered sequence without application of magnetization preparation modules (B). In the current illustration, each 3D radial spiral interleave is composed of 6 FISS modules (NR = 4), and each spiral is rotated by the golden angle (C). The stop and restart of the FISS sequence will lengthen the acquisition of a single 3D radial interleave compared to the use of a continuous uninterrupted bSSFP sequence (D). ECG, electrocardiogram; FISS, fast interrupted steady state; NR, number of readouts per FISS module; SI, superior-inferior

A typical FISS module starts with an α/2 tip-down pulse, followed by 180° phase-alternated RF excitation pulses for which the number depends on the number of readouts (NR) per FISS module, and it ends with an α/2 tip-up pulse (Figure 1A) according to the original implementation.[6] Each FISS module is followed by gradient spoilers, and RF spoiling is applied across different FISS modules using a 117° phase increment.[6] The repeated interruptions cause a sequence duration ($t_{sequence}$) increase compared with bSSFP, especially for lower values of NR, and can be estimated as follows:

$$t_{\text{sequence}} \approx (N_{\text{readouts}}/NR) * \left((NR+1) * TR + t_{\text{pulse}} + t_{\text{spoiler}}\right),$$

With $N_{readouts}$ defining the total number of readouts in a sequence, $t_{spoiler}$ the duration of the spoiler gradient, and t_{pulse} the RF excitation pulse duration. Sequence durations of bSSFP sequences can be estimated using an NR that approaches $N_{readouts}$.

2.2 | Pulse sequence implementation for 3D radial free-running FISS

A prototype 3D radial FISS sequence was implemented and integrated into a 5D compressed sensing whole-heart sparse MR imaging methodology.[4] FISS was programmed as a continuous sequence without magnetization preparation modules (Figure 1B).

As a basis for the FISS implementation, a free-running bSSFP sequence was used, which is a 3D radial sequence[1] that follows a spiral phyllotaxis k-space sampling pattern[9] rotated about the *z*-axis by the golden angle[10] (Figure 1C). The first readout of each radial interleave is oriented along the superior–inferior (SI) direction and is used for cardiac and respiratory self-gating.

The amount of spokes (i.e., k-space readouts per radial interleave) was fixed to keep a similar radial trajectory, as in refs. 1 and 4. Each 3D radial interleave contained a total of 24 spokes that can be divided into a flexible number of FISS modules allowing for NR = 1, 2, 3, 4, 6, 8, 12, 24. Non–slice-selective rectangular RF excitation pulses of 0.3 ms duration were used as opposed to earlier reported thin slab-selective RF excitation pulses.[6] A scan duration comparison was made between FISS and bSSFP using the vendor-provided sequence simulator and a TR of 3.0 ms.

2.3 | Numerical simulations

Numerical simulations of the Bloch equations were performed in MatLab 2018b (MathWorks, Natick, MA) to compute the transverse magnetization (M_{xy}) of FISS and bSSFP sequences for a range of resonance frequencies and sequence parameters, providing a quantitative comparison of signal suppression and suppression BW. Unless otherwise stated, simulations included rectangular RF excitation pulses of 0.3 ms duration, RF excitation angles of 40°, perfect RF and gradient spoiling between subsequent FISS modules by nulling M_{xy}, a T_1 of 1600 ms, and a T_2 of 180 ms as used before in ref. 6.

A first set of simulations was performed to compare M_{xy} (i.e., measured signal) of FISS and bSSFP sequences as a function of off-resonance and RF excitation angle. Off-resonance

varied between −500 Hz and 100 Hz (steps of 2 Hz); the RF excitation angles varied between 20° and 60° (steps of 1°); the NR was set to 1; and the TR was set to 3.0 ms.

In a second set of simulations, M_{xy} was determined as a function of TR and off-resonance to investigate the suppression BW, defined as the bottom 10% (i.e., a 10-fold reduction of fat signal) of the maximum on-resonant water M_{xy}. Tissue frequencies were varied between −500 Hz and 100 Hz (steps of 1 Hz) and the TR between 2.0 ms and 4.0 ms (steps of 0.05 ms). Simulations were repeated for NR = 1, 2, 3, 4, 6, 8, 12, 24.

Because these 2 simulations illustrate the FISS signal response only for precise tissue frequencies, a third set of simulations was performed to quantify a more realistic fat signal suppression as a function of TR and NR at 1.5T and 3T. Here, to simulate B_0 field inhomogeneity, the fat signal was defined as a normalized Gaussian spectrum with a FWHM of 50 Hz centered around −220 Hz (1.5T) or −440 Hz (3T). The M_{xy} of this spectrum was simulated by varying the TR from 2.0 ms to 4.0 ms (in steps of 0.05 ms) and by varying the NR from 1 to 24 (in steps of 1).

2.4 | Phantom experiments

Fat suppression capabilities were tested in baby oil (Johnson & Johnson, New Brunswick, NJ) on clinical 1.5T and 3T MRI systems (Magnetom Aera and Magnetom Prisma^{FIT}; Siemens Healthcare, Erlangen, Germany) with a FOV of $(220\ mm)^3$, matrix size of 112^3, and RF excitation angle of 40°. The TR was varied from the minimum TR possible, from 2.3 ms (1.5T) and 2.5 ms (3T) to 4.0 ms in steps of 0.1 ms, by varying the receiver BW. Experiments were repeated for NR = 1, 2, 3, 4, 6, 8, 12, 24. Scans using uninterrupted bSSFP without fat saturation were performed to ascertain the magnitude of fat signal suppression in FISS.

In a second experiment, with a FISS scan (NR = 8, TR = 3.0 ms), the effect of gradients spoilers was tested because they contribute significantly to the scan duration.

2.5 | 5D Whole-heart free-running FISS and bSSFP in volunteers

A free-breathing non–ECG-triggered 3D radial FISS sequence was used to perform whole-heart imaging in 10 volunteers. All experiments followed institutional guidelines, and all volunteers provided written informed consent. In each volunteer, a FISS and a bSSFP acquisition were performed, either at 1.5T or 3T (5 volunteers on each scanner). Imaging parameters for both sequences were as follows: FOV of $(220\ mm)^3$. The RF excitation angles were maximized at both field strengths to operate within the safety limits of the scanner, resulting in RF excitation angles of 40° to 45° at 3T and 50° to 60° at 1.5T. Whole-heart volumes were acquired with an isotropic spatial resolution of 1.1 mm^3 or 1.38 mm^3, respective matrix sizes of 192^3 and 160^3, and acquisition of 3419 or 5181 radial interleaves (with each 24 spokes), resulting in 82,056 or 124,344 acquired k-space lines. For experiments at 1.5T, the lowest possible TR was used, which varied from 2.75 ms to 3.0 ms and depended on the spatial resolution. At 3T, the TR was varied between 3.0 ms and 3.4 ms. The specific absorption rate that was provided on the user interface was recorded.

2.6 | Motion extraction and motion-resolved image reconstruction

The acquired 3D data were sorted into a 5D motion-resolved dataset that contains separate respiratory and cardiac dimensions as described previously.[4,5] Both respiratory and cardiac motion signals were extracted from the SI projections[9] acquired at the beginning of each radial interleave (Figure 1B).[3,11] The self-gating signals were used for data binning in the respiratory dimension with 4 motion states resolved from end-inspiration to end-expiration, and in the cardiac dimension with cycles temporally divided into windows of 50 ms width. 5D motion-resolved images were then reconstructed using XD-GRASP.[5]

2.7 | Data analysis

Phantom data and non–motion-resolved volunteer data reconstructed at the scanner were used to quantify SNR in compartments containing oil or chest fat by dividing the average signal of fat by the SD of the background signal outside the region of interest.

A cardiac volume at end-expiration and mid-diastole was selected for visual comparison of coronary vessel reformats obtained with SoapBubble.[12] In these reformats, coronary vessel sharpness was calculated along both the left anterior descending coronary artery and the right coronary artery.

A paired Student *t* test was performed on phantom and volunteer data. Results are represented as average ± 1 SD, and $P < 0.05$ was considered statistically significant.

3 | RESULTS

3.1 | FISS and bSSFP scan duration

The acquisition time of FISS is highly variable and depends on NR. Using a single readout per FISS module (NR = 1), the acquisition time of a single radial interleave increases by 205% compared to a non–fat-suppressed bSSFP sequence (Figure 1D). By increasing NR to 24, the relative acquisition time increase is 8% compared with bSSFP. Although high NR values may be favorable for scan time duration, they affect fat

suppression behavior. The relative scan time increase comparing FISS and non–fat-suppressed bSSFP for NE = 4 and NE = 8 is 53% and 26%, respectively (Figure 1D).

3.2 | Numerical simulations

FISS provides the same maximum on-resonant (~0 Hz) signal intensity compared with bSSFP for a similar range of RF excitation angles, but with FISS a broad suppression BW can be observed around −220 Hz and −440 Hz (Supporting Information Figure S1).

Numerical simulations show the effect of TR and off-resonance on the signal behavior for NR = 1, 4, and 8 (Figure 2; see also Supporting Information Figure S2 for the full range of NR that was simulated). NR influences the number of relatively narrow bands (with FWHM of ~10-20 Hz) that disrupt the suppression BW (Figure 2A,D,G).

In practical terms, concomitantly with increasing NR, these bands increase in frequency, which decreases the signal suppression BW while increasing the TR changes the location of the suppression bands. Increasing NR will reduce scan time on the one hand but also decreases the range of TR values that are adequate for fat suppression.

Because the ideal sequence would provide broad fat suppression with reasonable scan times, and considering the above findings, the following parameter combination is

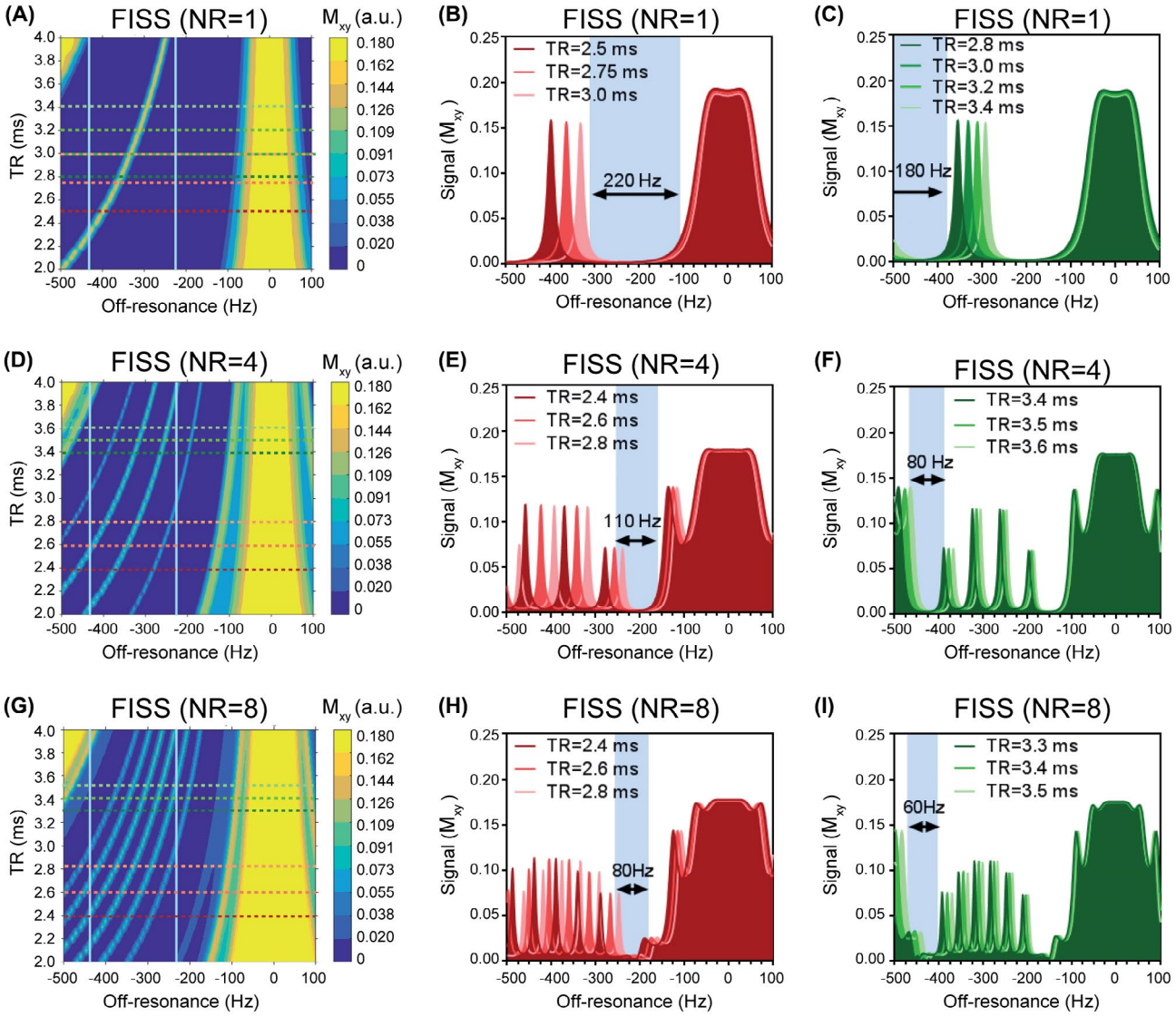

FIGURE 2 Bloch simulations of FISS illustrate the effect on M_{xy} as function of TR and off-resonance and simultaneously depicts the behavior for fat at 1.5T (−220 Hz) and 3T (−440 Hz). For NR = 1 (A, B, C), NR = 4 (D, E, F), and NR = 8 (G, H, I), different signal behavior can be observed. An increase in the number of readouts per FISS module (NR) mainly affects the width of the fat suppression bands, whereas a change in TR mainly affects the location of the bands. Simulations up to NR = 24 were performed (See Supporting Information Figure S2). The fat resonances at 1.5T and 3T are indicated by the vertical lines in (A, D, G). The horizontal green lines (in A, D, G) correspond to fat signal responses at 1.5T that match TR values (in B, E, H), and the red lines correspond to fat signal esponses at 3T that match TR values (in C, F, I). M_{xy}, transverse magnetization; T, tesla

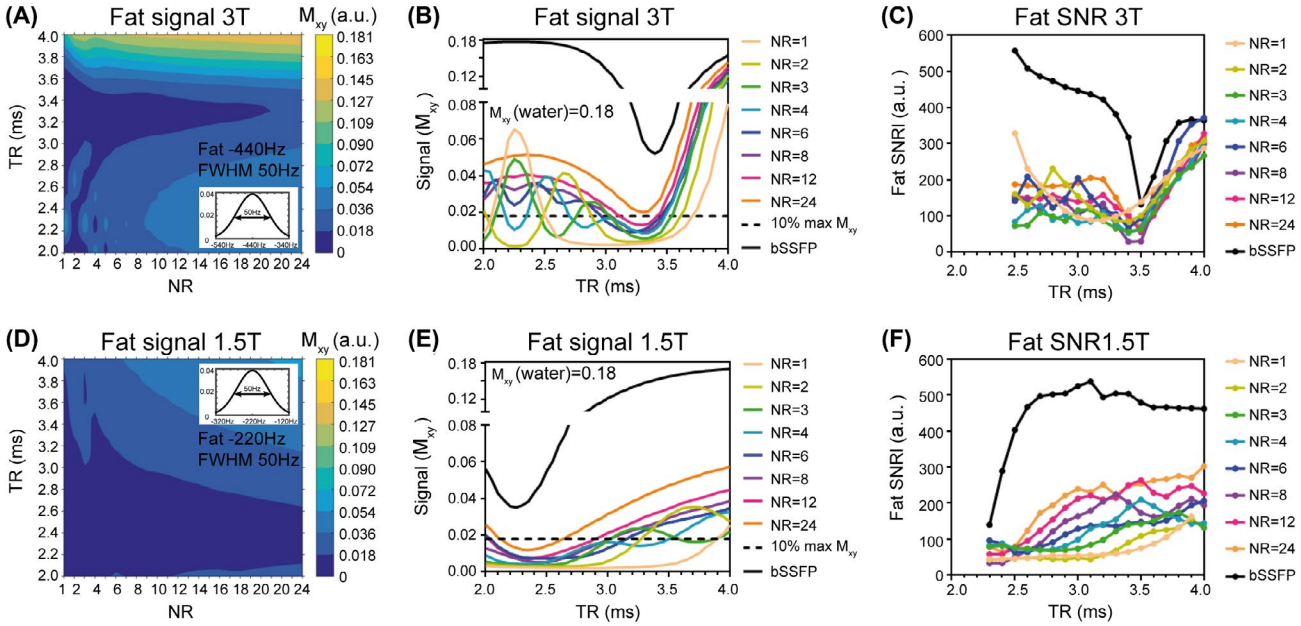

FIGURE 3 A fat profile consisting of a normalized gaussian distribution with an FWHM of 50 Hz around −440 Hz and −220 Hz was used to simulate the effect of TR and NR on M_{xy} (A, D). These plots were normalized to the maximum on-resonance (i.e., water) M_{xy}. Line plots demonstrate clearly the effect of NR on fat suppression as function of TR compared with bSSFP (B, E), and this signal behavior was corroborated by the experimental fat SNR observed in a baby oil phantom (C, F). The darkest blue region (in A, C) correspond to the bottom 10% of M_{xy} and corresponds to the region where fat is considered suppressed

proposed for use in 5D whole-heart free-running imaging: With NR = 8, at 1.5T, a TR in the range of 2.0 ms to 3.0 ms (~80 Hz suppression BW) (Figure 2G,H) should be chosen. At 3T, a TR in the range of 3.0 ms to 3.5 ms (~60 Hz BW) (Figure 2G,I) was deemed optimal.

Using a fat signal distribution mitigates the effect of the ~10 to 20 Hz excitation bands occurring at specific frequencies and contributes to a more intuitive understanding of applicable TR values. It can be seen that the total contributing fat signal at 3T drops to below 10% for TRs around 3.2 ms (Figure 3A). It also demonstrates that with NR = 4, fat suppression may be achievable with TRs of 2.7 ms, compared with 3 ms using NR = 2 or 3 (Figure 3B). This reveals that a FISS acquisition of NR = 4 poses a better candidate compared to NR = 2 or 3, allowing even shorter scan durations. At 1.5T, the range of possible TRs is wider when compared to that at 3T (Figure 3D); here, the simulation also suggests that a FISS acquisition with NR = 4 performs better compared with NR = 3 or 2 (Figure 3E).

3.3 | Phantom experiments

Phantom scans demonstrated a clear difference in fat suppression of FISS when compared to bSSFP, with FISS approaching bSSFP behavior with increasing NR. Fat SNR behavior in phantom experiments corresponded well with that of the simulations at both field strengths (Figure 3B,E and C,F).

No change in image quality was observed with and without the use of gradient spoilers (Supporting Information Video S1A,B); however, a clear signal fluctuation in SI projections was observed when spoilers were not applied (Supporting Information Video S1C,D). SI projections form a necessary component for accurate motion extraction, and thus gradient spoilers must be included.

3.4 | 5D Whole-heart free-running FISS and bSSFP in volunteers

Free-running FISS acquisitions were successfully performed in all volunteers. The specific absorption rate for free-running FISS was 92% (1.5T) and 94% (3T) of that of the uninterrupted bSSFP sequence, with 1.7 ± 0.6 watts (W)/kg (1.5T) and 1.9 ± 0.5 W/kg (3T) for FISS and 1.8 ± 0.6 W/kg (1.5T) and 2.0 ± 0.6 W/kg (3T) for bSSFP. As a reference for comparison, the average (N = 10) specific absorption rate for a triggered 3D Cartesian single-phase coronary MRI scan at 1.5T using the protocol in ref. 13 was 1.0 ± 0.1 W/kg. In general, a large difference in image quality was observed when comparing FISS to bSSFP (Figures 4-7), with the former demonstrating markedly reduced streak artifact. In all volunteers, overall fat SNR on FISS images relative to bSSFP was significantly decreased ($P < 0.01$) from 62.4 ± 30.0 to 25.6 ± 17.0 (Figure 7B).

The use of the free-running framework enabled a clear visualization of the different respiratory and cardiac motion

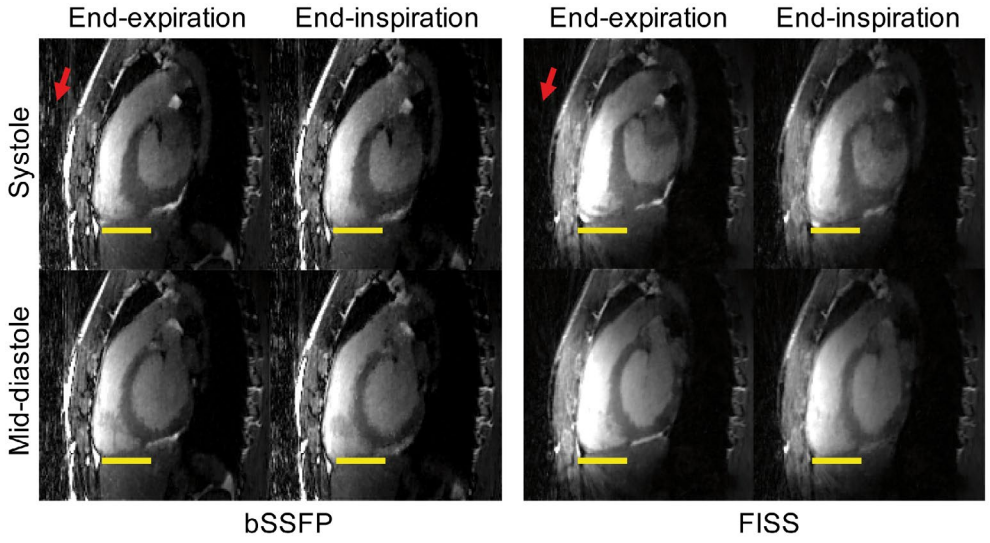

FIGURE 4 Comparison of 5D whole-heart images multiplanar reformatted in sagittal planes and acquired with free-breathing non ECG-triggered FISS (NR = 8) and bSSFP at 3T. Images are displayed in systole and mid-diastole, at both end-expiratory and end-inspiratory phases. Yellow lines serve to indicate the respiratory motion. Note the decrease in streaking artifacts in FISS compared with bSSFP indicated by the red arrows. The scan duration was 5:49 min for FISS (NR = 8, TR = 3.4 ms) and 4:39 min for bSSFP for an isotropic resolution of 1.38 mm^3. Motion can be better appreciated in an animation (see Supporting Information Video S2). bSSFP, continuous balanced steady-state free precession

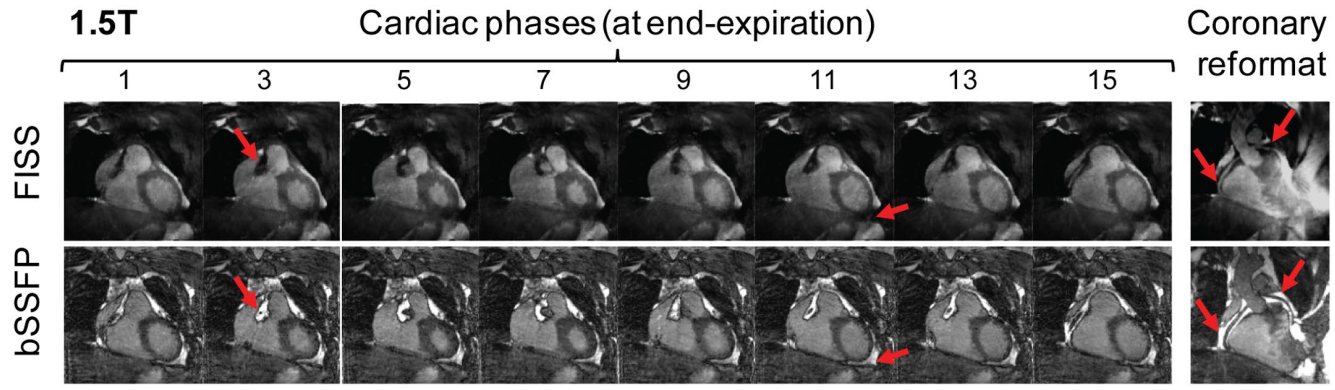

FIGURE 5 Comparison of 5D whole-heart images in coronal planes acquired with free-breathing non–ECG-triggered FISS and bSSFP at 1.5T. In this subject data was reconstructed using 16 cardiac phases and 4 respiratory phases. The displayed images correspond to the end-expiratory phase and only 8 out of 16 cardiac phases are shown. Scan time duration was 4:46 min for FISS (NR = 8, TR = 2.75 ms) and 3:45 min for bSSFP for an isotropic resolution of 1.38 mm^3. Red arrows indicate cardiac regions containing fat that is suppressed with FISS but not with bSSFP

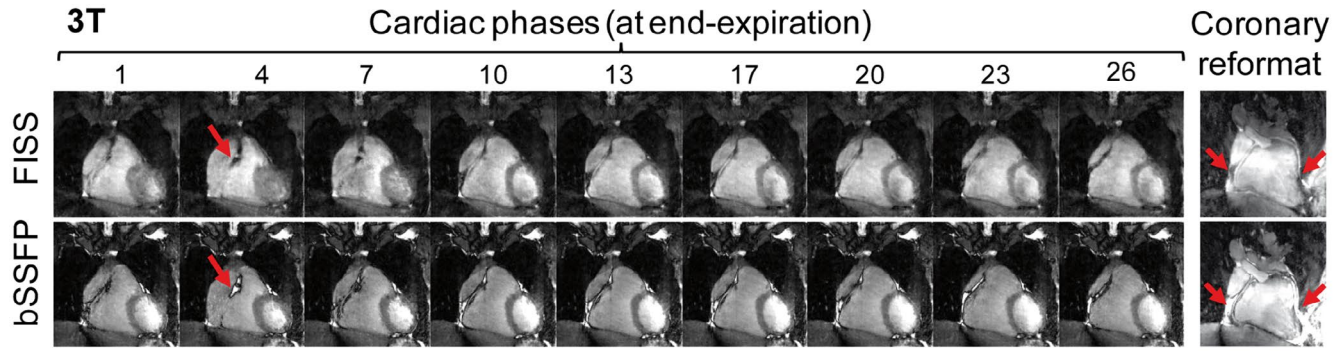

FIGURE 6 Comparison of 5D whole-heart images in coronal planes acquired with free-breathing non–ECG-triggered FISS and bSSFP at 3T. In this subject data was reconstructed using 26 cardiac phases and 4 respiratory phases. Only 7 out of 26 cardiac phases are shown, all at end expiration. Scan time duration was 6:20 min for FISS (NR = 4, TR = 3.0ms) and 4:08 min for bSSFP for an isotropic resolution of 1.38 mm^3. Red arrows indicate cardiac regions containing fat that is suppressed with FISS but not with bSSFP

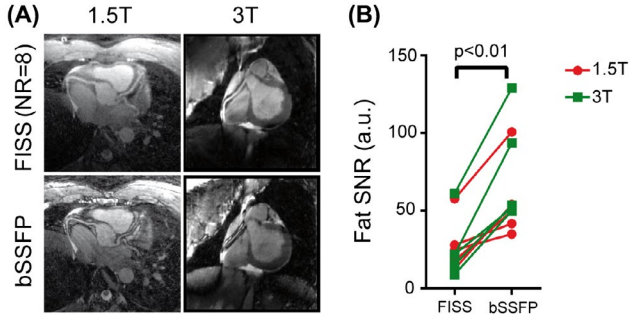

FIGURE 7 Comparison of coronary reformats obtained with FISS and bSSFP with an isotropic resolution of 1.1 mm^3 at 1.5 and 3T (A). The water–fat cancellation artifacts at the coronary vessel borders can be clearly observed in the bSSFP scans. The scan time duration at 1.5T was 7:53 min for FISS (NR = 8, TR = 3.0 ms) and 6:19 min for bSSFP. At 3T, the scan time duration was 8:45 min for FISS (NR = 8, TR = 3.4 ms) and 7:00 min for bSSFP. The SNR of fat was determined in non–motion-resolved images and was significantly decreased in FISS compared with bSSFP

states using both FISS and bSSFP acquisitions (Figure 4). On FISS images, fat signal originating from the chest was visibly lower when compared with bSSFP (Figures 4-7), which is consistent with the reduced level of streaking artifacts.

Coronary arteries were also successfully visualized in some of the reconstructed cardiac phases in coronal views (Figures 5,6) and can be better delineated in the reformats (Figures 5-7A), where a strong water–fat cancellation artifact can be observed at the vessel borders using bSSFP but not FISS and is independent of the magnetic field strength. Vessel sharpness of the right coronary artery and left anterior descending coronary artery was higher in bSSFP compared with FISS, from 42% ± 12% to 31% ± 9% (right coronary artery, $P = 0.06$) and from 50% ± 5% to 38% ± 7% (left anterior descending coronary artery, $P = 0.04$) (Supporting Information Figure S3). The scan durations of the free-running FISS acquisitions depended on NR, TR, and resolution and varied between 4:46 min (NR = 8, TR = 2.75, 1.38 mm^3 resolution, 3:45 min for bSSFP) and 9:26 min (NR = 4, TR = 3.0 ms, 1.1 mm^3 resolution, 6:19 for bSSFP). Note that when using the free-running framework, the scan time is no longer dependent on respiration or cardiac frequency.

4 | DISCUSSION

In this study, a 3D radial FISS sequence was implemented as part of a 5D whole-heart free-running framework. The capabilities of the sequence in terms of fat suppression with respect to bSSFP was demonstrated in simulations and phantoms, and a full range of sequence parameters for fat suppression at both 1.5T and 3T was provided. Consistent with these findings, 5D whole-heart free-running FISS showed promising results for motion-resolved whole-heart imaging and its potential for nonenhanced MRA at both 1.5T and 3T that comes with only a modest increase in scan time compared with non–fat-suppressed bSSFP. For comparison, and if fat saturation and ramp-up pulses were inserted to provide for fat suppression in bSSFP, the scan time would be 14 min,[1,4] which is 80% higher than that of FISS (7 min 49 s) with NR = 8 and a TR of 3 ms.

The FISS protocol was optimized in simulations using NR values up to 24, and the relationship between this parameter and fat suppression BW was elucidated in detail. Phantom results were consistent with simulations and demonstrated that fat signal suppression is effective for a wide range of NR and showed decreased fat suppression compared to bSSFP. Clearly, the range in TR for which effective fat suppression can be obtained is constrained. In addition, the numerical simulations predicted a more effective fat signal reduction than was observed in vitro (Figure 3). This may be attributed to the fact that undersampling artifacts in radial imaging increases the background noise level, especially when fat is not entirely suppressed. Secondly, in these experiments the TR was changed by changing the receiver BW, which may also have an effect on SNR. However, using the plots derived from numerical simulations and phantom experiments in this study, it is now possible to prescribe the TR that leads to maximized in vivo fat suppression for different NRs and for both 1.5T and 3T.

The free-running FISS protocol was optimized based on simulations and achieved a reduced fat signal and reduced streak artifact following a motion-resolved reconstruction approach when compared to an equivalent free-running bSSFP protocol without fat suppression. Clearly, the level of fat suppression obtained with FISS enables the visualization of small anatomical structures such as the coronary arteries. FISS also produced comparable cardiac images with respect to bSSFP in terms of signal and motion without using contrast agents. B_0 variations across the heart are on the order of 35 to 60 Hz[14] and therefore are not expected to be a problem for FISS with a broad trough in the region of fat frequencies, which is consistent with the observation of fat suppression in the cardiac images. The occurrence of water–fat cancellation artifacts with bSSFP could be clearly observed at the vessel borders and resulted in increased vessel sharpness in the uninterrupted bSSFP scans compared with FISS. When fat saturation is inadequate, water–fat cancellation artifacts may still be observed, as was the case in some of the vessel borders displayed in previous fat-suppressed free-running bSSFP approaches at 1.5T[1,4] but not on FISS as investigated here. A decrease in vessel border sharpness in the absence of water–fat cancellation contributed to a perceived visual blurring of FISS images compared with bSSFP.

In terms of scan time compared with previous free-running approaches, the GRE free-running approach at 3T had

a reported scan duration of 10 min and necessitated the use of contrast agents, whereas that of the fat-suppressed bSSFP counterpart at 1.5T led to 14 min scanning time. The relatively long scan duration of free-running bSSFP was caused by the mandatory ramp-up pulses applied after each fat saturation pulse[1,4] and in free-running GRE by lengthy water excitation pulses resulting in longer TRs.[2] Compared to conventional fat suppression,[15] water excitation pulses[16] would not interrupt the steady state in bSSFP but may increase the TR. Even the use of relatively short water excitation pulses such as lipid insensitive binomial off-resonant RF excitation (LIBRE)[17-19] would prolong the TR by some extent. Therefore, the current free-running FISS implementation may provide an effective alternative at both field strengths.

In the recently reported 2D radial cine FISS sequence protocols, NR values ranging from 1 to 8 were used.[6,7] In the current study, 5D whole-heart free-running FISS was performed using either NR = 4 or NR = 8. In our specific use case, this divides the spiral interleave consisting of 24 lines into 6 or 3 FISS modules. A limitation of FISS is that it still increases scan time compared with a continuous albeit non–fat-suppressed bSSFP acquisition. Future studies may investigate the utility of higher NR values or a lower number of acquired k-space lines per spiral interleave, which were not investigated in this study but may further decrease scan time. The application of a gradient spoiler increased the scan time but was critical for the acquisition of stable SI projections aimed at a total self-gated respiratory and cardiac motion extraction. The gradient spoiler strength and duration was not optimized, but this may help reduce the scan time further. Using pilot-tone navigation[20] motion extraction would no longer rely on stable SI projections and may be omitted from the sequence together with the gradient-spoilers. Lastly, further improvements in fat suppression may be achieved by tuning the TR in a patient-specific way by incorporating a detailed fat spectrum analysis. A comparison with alternative fat saturation approaches, including chemical shift selective suppression plus ramp-up pulses or water excitation pulses, was not performed in the current study. However, the free-running bSSFP approach described in refs. 1 and 4 would only have been feasible at 1.5T, and the free-running GRE approach described in ref. 2 only at 3T with the use contrast agents. Lastly, the clinical utility and impact of the proposed free-running sequence was not investigated in the current study and will be the subject of future investigations.

The proposed 5D whole-heart free-running FISS approach offers native fat suppression and reduced streak artifact with a modest (~25%) increase in scan duration when compared to non–fat-suppressed bSSFP. Cardiac MRI examinations are typically challenging because of the complex anatomy of the heart, the epicardial fat, and both the need for large volumetric coverage and adequate motion suppression. Using a 5D motion-resolved imaging approach that incorporates fat suppression, these issues can be addressed, and patient setup time and scan planning are substantially abbreviated because both ECG lead placement and scan plane positioning are no longer needed.

5 | CONCLUSION

3D radial FISS was implemented and optimized using numerical simulations and phantom studies, and it demonstrated highly effective fat suppression and reduced streak artifact with modest scan time increases compared to non–fat-suppressed bSSFP. The integration of 3D radial FISS in a free-running framework enabled natively fat-suppressed fully self-gated respiratory and cardiac motion resolved whole-heart imaging at both 1.5T and 3T, and its feasibility for noncontrast coronary angiography was demonstrated.

ACKNOWLEDGMENT

J.A.M.B. received funding from the Swiss National Science Foundation (grant number PZ00P3_167871), the Emma Muschamp Foundation, and the Swiss Heart Foundation. M.S. received funding from the Swiss National Science Foundation (grant numbers 173129, 150828, and 143923). R.R.E. received funding from the National Institutes of Health (grant numbers R01 HL130093 and R01 HL137920). I.K. received funding from the National Institutes of Health (grant number R01 EB027475). J.A.M.B. designed the study, developed and implemented the sequence, performed the simulations, acquired and analyzed the data, and wrote the manuscript. D.P. contributed the sequence code for free-running and contributed to the study design. L.D.S. provided the self-gating code; C.W.R. and J.H. contributed to the data acquisition; I.K. and R.R.E. provided sequence code snippets for FISS; J.Y. provided the 5D reconstruction framework; and M.S. contributed to the study design and drafting of the manuscript. All authors read and revised the manuscript.

CONFLICT OF INTEREST

Davide Piccini is an employee of Siemens Healthcare.

ORCID

Jessica A.M. Bastiaansen https://orcid.org/0000-0002-5485-1308
Davide Piccini https://orcid.org/0000-0003-4663-3244
Lorenzo Di Sopra https://orcid.org/0000-0003-3426-9457
John Heerfordt https://orcid.org/0000-0002-6837-4733
Robert R. Edelman https://orcid.org/0000-0002-0013-8822
Matthias Stuber https://orcid.org/0000-0001-9843-2028

REFERENCES

1. Coppo S, Piccini D, Bonanno G, et al. Free-running 4D whole-heart self-navigated golden angle MRI: initial results. *Magn Reson Med*. 2015;74:1306–1316.
2. Pang J, Sharif B, Fan Z, et al. ECG and navigator-free four-dimensional whole-heart coronary MRA for simultaneous visualization of cardiac anatomy and function. *Magn Reson Med*. 2014;72:1208–1217.
3. Disopra L, Piccini D, Coppo S, Bastiaansen JAM, Stuber M, Yerly J. Motion-resolved 5D imaging of the heart: time to get rid of the ECG? In Proceedings of the 25th Annual Meeting of ISMRM, Honolulu, HI, 2017. p. 3148.
4. Feng LI, Coppo S, Piccini D, et al. 5D whole-heart sparse MRI. *Magn Reson Med*. 2018;79:826–838.
5. Feng L, Axel L, Chandarana H, Block KT, Sodickson DK, Otazo R. XD-GRASP: golden-angle radial MRI with reconstruction of extra motion-state dimensions using compressed sensing. *Magn Reson Med*. 2016;75:775–788.
6. Koktzoglou I, Edelman RR. Radial fast interrupted steady-state (FISS) magnetic resonance imaging. *Magn Reson Med*. 2018;79:2077–2086.
7. Edelman RR, Serhal A, Pursnani A, Pang J, Koktzoglou I. Cardiovascular cine imaging and flow evaluation using fast interrupted steady-state (FISS) magnetic resonance. *J Cardiovasc Magn Reason*. 2018;20:12.
8. Hennig J, Speck O, Scheffler K. Optimization of signal behavior in the transition to driven equilibrium in steady-state free precession sequences. *Magn Reson Med*. 2002;48:801–809.
9. Piccini D, Littmann A, Nielles-Vallespin S, Zenge MO. Respiratory self-navigation for whole-heart bright-blood coronary MRI: methods for robust isolation and automatic segmentation of the blood pool. *Magn Reson Med*. 2012;68:571–579.
10. Piccini D, Littmann A, Nielles-Vallespin S, Zenge MO. Spiral phyllotaxis: the natural way to construct a 3D radial trajectory in MRI. *Magn Reson Med*. 2011;66:1049–1056.
11. Di Sopra L, Piccini D, Coppo S, Stuber M, Yerly J. An automated approach to fully self-gated free-running cardiac and respiratory motion-resolved 5D whole-heart MRI. *Magn Reson Med*. 2019;82:2118–2132.
12. Etienne A, Botnar RM, Van Muiswinkel AM, Boesiger P, Manning WJ, Stuber M. "Soap-Bubble" visualization and quantitative analysis of 3D coronary magnetic resonance angiograms. *Magn Reson Med*. 2002;48:658–666.
13. Heerfordt J, Piccini D, Stuber M. A quantitative comparison of navigator-gated Cartesian and self-navigated radial free-breathing 3D bSSFP whole-heart coronary MRA. In: Proceedings of the Society for Cardiovascular Magnetic Resonance, Barcelona, Spain, 2018. p. 372044.
14. Schär M, Vonken E-J, Stuber M. Simultaneous B(0)- and B(1)+-map acquisition for fast localized shim, frequency, and RF power determination in the heart at 3 T. *Magn Reson Med*. 2010;63:419–426.
15. Haase A, Frahm J, Hanicke W, Matthaei D. H-1-Nmr Chemical-Shift Selective (Chess) Imaging. *Phys Med Biol*. 1985;30:341–344.
16. Hore PJ. Solvent suppression in Fourier-transform nuclear magnetic-resonance. *J Magn Reason*. 1983;55:283–300.
17. Bastiaansen JAM, Stuber M. Flexible water excitation for fat-free MRI at 3T using lipid insensitive binomial off-resonant RF excitation (LIBRE) pulses. *Magn Reson Med*. 2018;79:3007–3017.
18. Colotti R, Omoumi P, van Heeswijk RB, Bastiaansen JAM. Simultaneous fat-free isotropic 3D anatomical imaging and T2 mapping of knee cartilage with lipid-insensitive binomial off-resonant RF excitation (LIBRE) pulses. *J Magn Reson Imaging*. 2019;49:1275–1284.
19. Bastiaansen JAM, van Heeswijk RB, Stuber M, Piccini D. Noncontrast free-breathing respiratory self-navigated coronary artery cardiovascular magnetic resonance angiography at 3 T using lipid insensitive binomial off-resonant excitation (LIBRE). *J Cardiovasc Magn Reason*. 2019;21:38.
20. Bacher M, Speier P, Bollenbeck J, Fenchel M, Stuber M. Pilot tone navigation enables contactless prospective cardiac triggering: initial volunteer results for prospective cine. In Proceedings of the 26th Annual Meeting of ISMRM, Paris, France, 2018. p. 4798.

SUPPORTING INFORMATION

Additional supporting information may be found online in the Supporting Information section at the end of the article.

FIGURE S1 Bloch simulations of bSSFP (A) and FISS (NR = 1) (B) were performed to compare the transverse magnetizations as function of off-resonance and RF excitation angle. Both with bSSFP and FISS, the top 10% of M_{xy} can be obtained within a similar RF excitation angle range. FISS provides the same maximum on-resonant (~0 Hz) signal intensity compared with bSSFP. However, a broad fat suppression bandwidth with NR = 1 can be observed around −220 Hz and −440 Hz, while bSSFP displays a narrow band, occurring as expected at frequencies of 1/TR

FIGURE S2 Bloch simulations of FISS illustrate the effect on the transverse magnetization as function of TR and off-resonance. For NR = 1 to NR = 24. An increase in the number of readouts per FISS module (NR) mainly affects the width of the fat suppression bands, while a change in TR mainly affects the location of the bands. The white arrows indicate regions of fat suppression for either −440 Hz or −220 Hz which corresponds to the frequency of fat at 3T or 1.5T respectively

FIGURE S3 Coronary vessel sharpness was computed to compare whole-heart free-running FISS and uninterrupted bSSFP for coronary MRA. The water-fat cancellation observed in voxels containing both water and fat introduces dark edges in bSSFP, which makes bSSFP look sharper

VIDEO S1 The image quality of a 3D FISS acquisition in a phantom is similar with and without the use of gradients

spoilers (A,B). However, the SI projections are not consistent without using gradient spoilers (C). Applying gradient spoilers stabilizes the SI projections (D) which is important for motion signal extraction

VIDEO S2 Animation showing cardiac and respiratory motion from data acquired with free-running FISS and bSSFP. Data corresponds to the same volunteer images shown in Figure 4 of the manuscript

How to cite this article: Bastiaansen JAM, Piccini D, Di Sopra L, et al. Natively fat-suppressed 5D whole-heart MRI with a radial free-running fast-interrupted steady-state (FISS) sequence at 1.5T and 3T. *Magn Reson Med*. 2020;83:45–55. https://doi.org/10.1002/mrm.27942